PHYSICAL REVIEW C, VOLUME 65, 034302

Isoscalar giant resonances in ^{28}Si and the mass dependence of nuclear compressibility

D. H. Youngblood, Y.-W. Lui, and H. L. Clark
Cyclotron Institute, Texas A&M University, College Station, Texas 77840
(Received 3 August 2001; published 5 February 2002)

The giant resonance region from 8 MeV$<E_x<$55 MeV in ^{28}Si has been studied with inelastic scattering of 240 MeV α particles at small angles including 0°. Strength corresponding to 81±10%, 68±9%, and 15±4% of the isoscalar $E0$, $E2$, and $E1$ sum rules, respectively, was identified with centroids of 21.25±0.38 MeV, 18.54±0.25 MeV, 19.15±0.60 MeV, and rms widths of 6.4±0.6 MeV, 4.7±0.6 MeV, and 6.9±0.7 MeV. The mass dependence of the compression modulus of finite nuclei is shown to be reasonably well reproduced from $A=24$ to 208 in relativistic mean field calculations with the NLC interaction having $K_{nm}=225$ MeV and in nonrelativistic calculations with the RATP interaction having $K_{nm}=240$ MeV.

DOI: 10.1103/PhysRevC.65.034302 PACS number(s): 25.55.Ci, 24.30.Cz, 27.30.+t

INTRODUCTION

The location of the isoscalar giant monopole resonance (GMR) is important because its energy can be directly related to the nuclear compressibility. There is much current interest in exploring the behavior of the nuclear equation of state as one moves away from stability, however, a relevant test of effective interactions that are used to obtain the equation of state is also how well they describe the compressibility (and hence the GMR) in stable nuclei over a wide range of A. Until recently the majority of the $E0$ strength in light nuclei was still unidentified, therefore the calculations could be tested only from $A=90$ to $A=208$, but even in this region the mass dependence of the GMR energy was not well reproduced [1]. In the last several years, however, the experimental situation has improved considerably, with much more precise data for the GMR in heavy nuclei [2] and the location of most of the GMR strength in several lighter nuclei [3–5]. There were a number of calculations with various interactions, both relativistic and nonrelativistic in the period 1995–1998, just before the new data became available. Comparing the new GMR data from ^{40}Ca to ^{208}Pb [2] to these calculations, the Hartree-Fock (HF) random phase approximation, (RPA) calculations of Blaizot *et al.* [1] using the Gogny interaction fit the mass dependence of the GMR energy quite well and this led to the conclusion that a Gogny interaction with $K_{nm}=231\pm5$ MeV was consistent with the data.

Now that most of the $E0$ strength has been identified in nuclei as light as ^{24}Mg [5], it is of interest to explore how various calculations predict the compressibility of nuclei over the range from ^{24}Mg to ^{208}Pb. The compressibility of a finite nucleus is related to the GMR energy by [6] $K_A=[M/\hbar^2]\langle r^2\rangle E_{\mathrm{GMR}}{}^2$ where in the scaling model $E_{\mathrm{GMR}}=(m_3/m_1)^{1/2}$ and $m_n=\langle E_x|r^2|0\rangle E_x{}^n$ is the nth moment of the strength distribution. K_A is affected not only by the bulk matter compressibility, but also by Coulomb, surface, symmetry, and other smaller effects. These have been parametrized in the Leptodermous expansion [6,7] $K_A=K_v+K_{sf}/A^{1/3}+K_{vs}\ [(N-Z)/A]+K_{\mathrm{Coul}}\ Z^2A^{-4/3}+$smaller terms. It has been shown by several authors [1,6,8] that these parameters cannot be obtained unambiguously from fitting to GMR data, however, Chossy and Stocker [9] have calculated these parameters for a number of interactions in the relativistic mean field while Nayak *et al.* [10] have calculated them with nonrelativistic Skyrme and other interactions. Hence these interactions can be tested with the recent data. Also Wang, Chung, and Santiago [11] have calculated GMR energies for ^{16}O to ^{208}Pb in the Thomas-Fermi model and have also calculated the Leptodermous parameters in this model.

Recently, 97±11% of the $E0$ energy-weighted sum rule (EWSR) has been identified in ^{40}Ca [4] and 72±10% found in ^{24}Mg [5], however only 54±6% of the $E0$ strength has been located in ^{28}Si [3] and 48±10% was located [12] in ^{16}O. We report here a further study of ^{28}Si where data were obtained with considerably better statistics, the folding model was used to obtain multipole strengths, and a new analysis procedure [4] was used which treats the continuum in a more consistent manner and allows extraction of multipole distributions with much better resolution.

EXPERIMENTAL TECHNIQUE AND RESULTS

The experimental technique has been described thoroughly in Ref. [5] and is summarized briefly below. A beam of 240 MeV α particles from the Texas A&M K500 superconducting cyclotron bombarded a self-supporting natural Si wafer 7.92 mg/cm^2 thick located in the target chamber of the multipole-dipole-multipole spectrometer. The horizontal acceptance of the spectrometer was 4° and ray tracing was used to reconstruct the scattering angle. The vertical acceptance was set at ±2°. The focal plane detector covered approximately 45 MeV of excitation and measured position and angle in the scattering plane. The out-of-plane scattering angle was not measured. Position resolution of approximately 0.9 mm and scattering angle resolution of about 0.09° were obtained. Cross sections were obtained from the charge collected, target thickness, dead time, and known solid angle. The cumulative uncertainties in target thickness, solid angle, etc., result in about a ±10% uncertainty in absolute cross sections.

Sample spectra obtained are shown in Fig. 1. The giant resonance peak can be seen extending up past $E_x=35$ MeV. The spectrum was divided into a peak and a continuum where the continuum was assumed to have the shape of a straight line at high excitation joining onto a Fermi

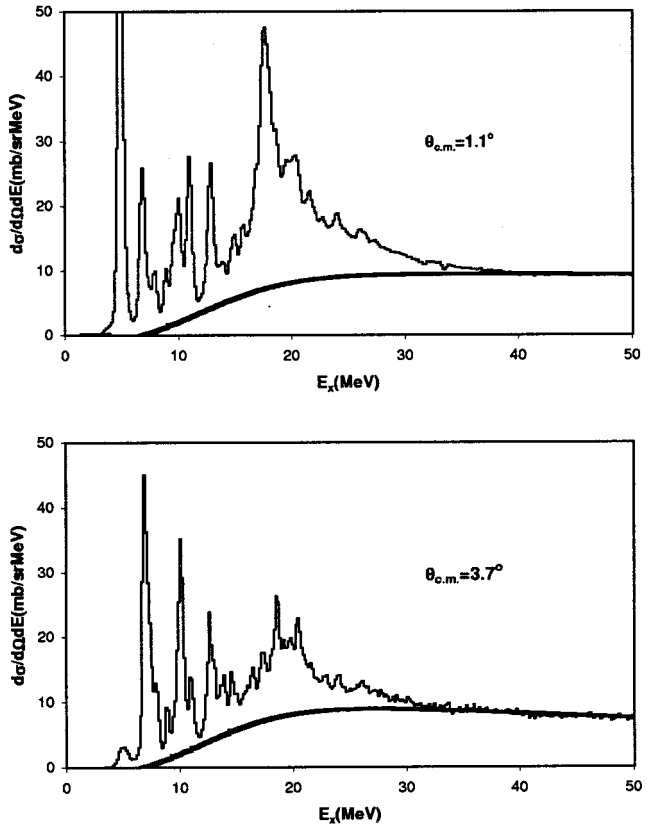

FIG. 1. Inelastic α spectra obtained for 240 MeV α particles on ^{28}Si at two angles. The thick lines show the continuum chosen for the analysis.

shape at low excitation [Eq. (1)] to model particle threshold effects:

$$Y(\text{continuum}) = A + B^{\star}E_x + Y_0^{\star}\{1+\exp[(E_x - E_{\text{th}})/C]\}. \quad (1)$$

A and B are determined from a fit to the high excitation region ($E_x = 42$ to 51 MeV), E_{th} and C are adjusted to model the behavior of the spectrum near the particle threshold, and Y_0 is adjusted so that the continuum obtained is zero in the region just below the particle threshold ($E_x = 6$ to 7 MeV). The parameters E_{th} and C were fixed to be the same for all spectra, while A, B, and Y_0 were required to change continuously as a function of angle for all spectra taken at the same spectrometer angle. The continua used are shown in Fig. 1.

The multipole components of the giant resonance peak were obtained [4,5] by dividing the peak into multiple regions (bins) by excitation energy and then comparing the angular distributions obtained for each of these bins to distorted wave Born approximation (DWBA) calculations to obtain the multipole components. The uncertainty from the multipole fits was determined for each multipole by incrementing (or decrementing) that strength, then adjusting the strengths of the other multipoles to minimize total χ^2. This continued until the new χ^2 was 1 unit larger than the total χ^2 obtained for the best fit.

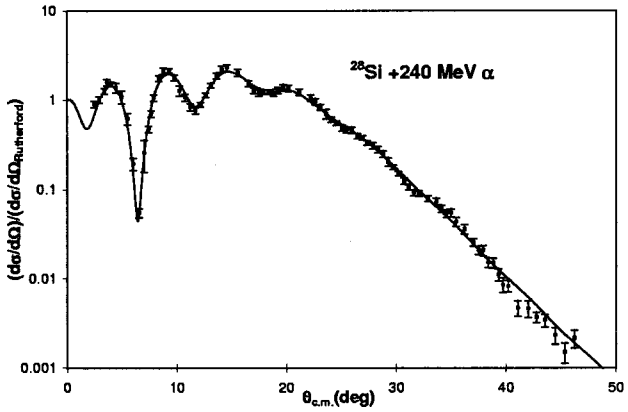

FIG. 2. Angular distribution of the ratio of the differential cross section for elastic scattering to Rutherford scattering for 240 MeV α particles from Si [3] is plotted versus average center-of-mass angle. The solid line shows an optical model calculation with the parameters from Table I.

The deformed potential model was used for the DWBA calculations reported in Ref. [3], however, Beene *et al.* [13] have shown that consistent agreement between electromagnetic transition strengths and those measured with light and heavy ion inelastic scattering for low lying 2^+ and 3^- states can only be obtained using the folding model. Therefore for this work we have used density dependent single folding with a Woods-Saxon imaginary term (DDWS) which was shown by Satchler and Khoa [14] to give excellent results for low lying states in ^{58}Ni excited by 240 MeV inelastic α scattering. In Ref. [5] it was shown that a DDWS analysis also gave excellent agreement with electromagnetic transition rates for discrete states in ^{24}Mg. Folding parameters were obtained by fitting the elastic scattering data reported in Ref. [1]. The fit to the elastic scattering is shown in Fig. 2 and the parameters are given in Table I. The transition densities and sum rules are described thoroughly in Refs. [2], [14], [15] and the values obtained for 100% of the sum rules in ^{28}Si for each multipolarity are given in Ref. [3]. It should be pointed out that the transition density given by Harakeh and Dieprink [15] for the isoscalar dipole resonance (ISGDR) in their Eq. (4) is for only one of the magnetic substates and must be multiplied by $(2l+1)^{1/2}$ to represent excitation of the ISGDR by α particles. DDWS calculations

TABLE I. Folding model and Fermi parameters used.

V (MeV)	W (MeV)	R_i (fm)	a_i (fm)	R_c (fm)	c (fm)	a (fm)
44.0	32.5	4.303	0.687	3.970	3.155	0.623

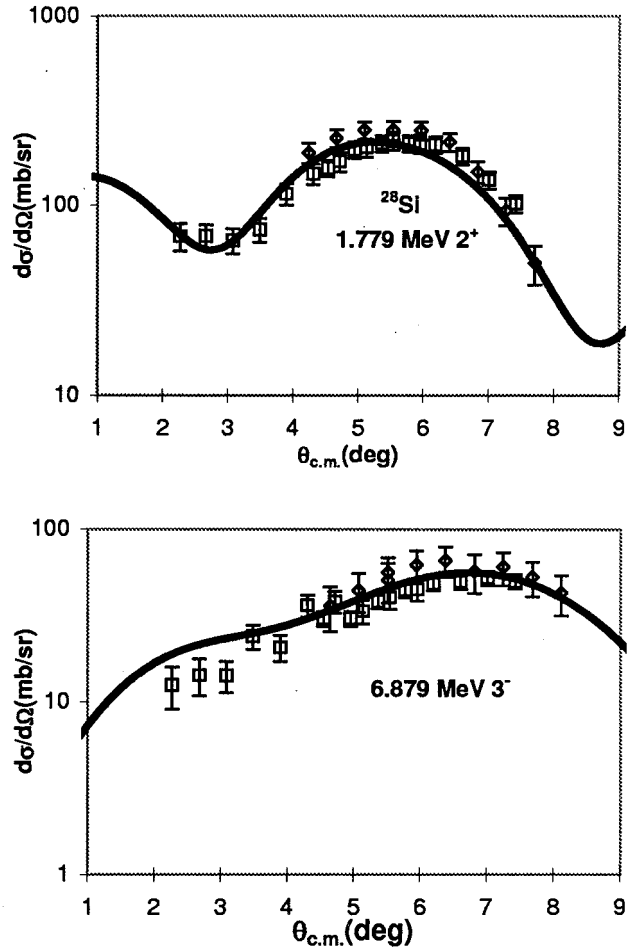

FIG. 3. (Top) Angular distribution of the differential cross section for inelastic alpha scattering to the 1.779 MeV 2^+ state in ^{28}Si plotted versus average center-of-mass angle. Data for two experimental runs are shown by the squares and diamonds. The solid line shows an $L=2$ DWBA calculation for the accepted B ($E2$) value [16]. (Bottom) Angular distribution of the differential cross section for inelastic α scattering to the 6.879 MeV 3^- state in ^{28}Si plotted versus average center-of-mass angle. Data for two experimental runs are shown by the squares and diamonds. The solid line shows an $L=3$ DWBA calculations for the accepted B ($E3$) value [16].

for the 1.779 MeV 2^+ and 6.879 MeV 3^- states in ^{28}Si using electromagnetic B(EL) values from the NNDC [16] are shown superimposed on data obtained for those two states in Fig. 3. The agreement is excellent. There is an 6.888 MeV 4^+ state unresolved from the 6.879 MeV state, but the calculated cross section for this state is small compared to the 3^- state. A comparison of the deformed potential calculations from Ref. [3] and the DDWS folding calculations for giant resonance excitations is given in the last column of Table II, where the cross sections at the peak of the respective multipole distributions at $E_x=18$ MeV are compared. In every case the DDWS cross section is smaller with the difference ranging from 17% for $E0$ to 85% for $E3$.

Samples of the angular distributions obtained for the giant resonance (GR) peak and the continuum are shown in Fig. 4. Fits to the angular distributions were carried out with a sum of isoscalar 0^+, 1^-, 2^+, 3^-, and 4^+ strengths. The isovector giant dipole resonance (IVGDR) contributions are small, but were calculated from the known distribution [17] and held fixed in the fits. Sample fits obtained, along with the individual components of the fits, are shown superimposed on the data in Fig. 4. $E3$ and $E4$ strength could not always be reliably distinguished due to the limited angular range of the experiment. The continuum angular distributions are similar over the entire energy range and can be fit primarily by a sum of $E1$, $E2$, and $E3$ angular distributions with small amounts of $E0$ strength below $E_x=27$ MeV. The $E0$ strength extracted from the continuum data represents $6\pm1\%$ of the $E0$ EWSR and, while the uncertainties are large, no contribution to $E0$ strength was found from the continuum above $E_x=27$ MeV. In the analysis reported in Ref. [3], the $E0$ strength necessary to fit the angular distributions of the continuum increased at higher excitation energy, however, that result was an artifact caused by the use (for all energies) of angular distributions calculated at only one energy. The energy dependence of the cross section was included by renormalization. This was a limitation of the fitting code used at the time. As can be seen in Fig. 4, the actual angular distributions change somewhat as excitation energy changes, particularly at the smallest angles. This limitation was removed in the later analyses of ^{24}Mg [5] and ^{40}Ca [4], where it was demonstrated that $E0$ strength in the peak and continuum could be identified, and that the total $E0$ strength obtained does not depend strongly on the continuum choice. The strengths of the other multipoles required to fit the continuum increase almost monotonically up to the highest excitation observed. Clearly reaction mechanisms other than multipole transitions are responsible for a significant part of the continuum and thus higher multipole components cannot be extracted reliably from the continuum in this manner. This is very similar to the result reported for ^{24}Mg [5].

The $E0$ distribution obtained from the peak plus the continuum and the (isoscalar) $E1$ and $E2$ multipole distributions obtained from the peak are shown in Fig. 5 and the results are summarized in Table II. The strength distributions ob-

TABLE II. Multipole parameters obtained for ^{28}Si.

	m_1/m_0 (MeV)	$(m_3/m_1)^{1/2}$ (MeV)	rms width (MeV)	%EWSR	Ratio def.pot./folding
$E0$	21.25 ± 0.38	23.7 ± 0.7	6.4 ± 0.6	81 ± 10	1.17
$E2$	18.54 ± 0.25		4.7 ± 0.6	68 ± 9	1.24
$E1(T=0)$	19.15 ± 0.60		6.9 ± 0.7	15 ± 4	1.37

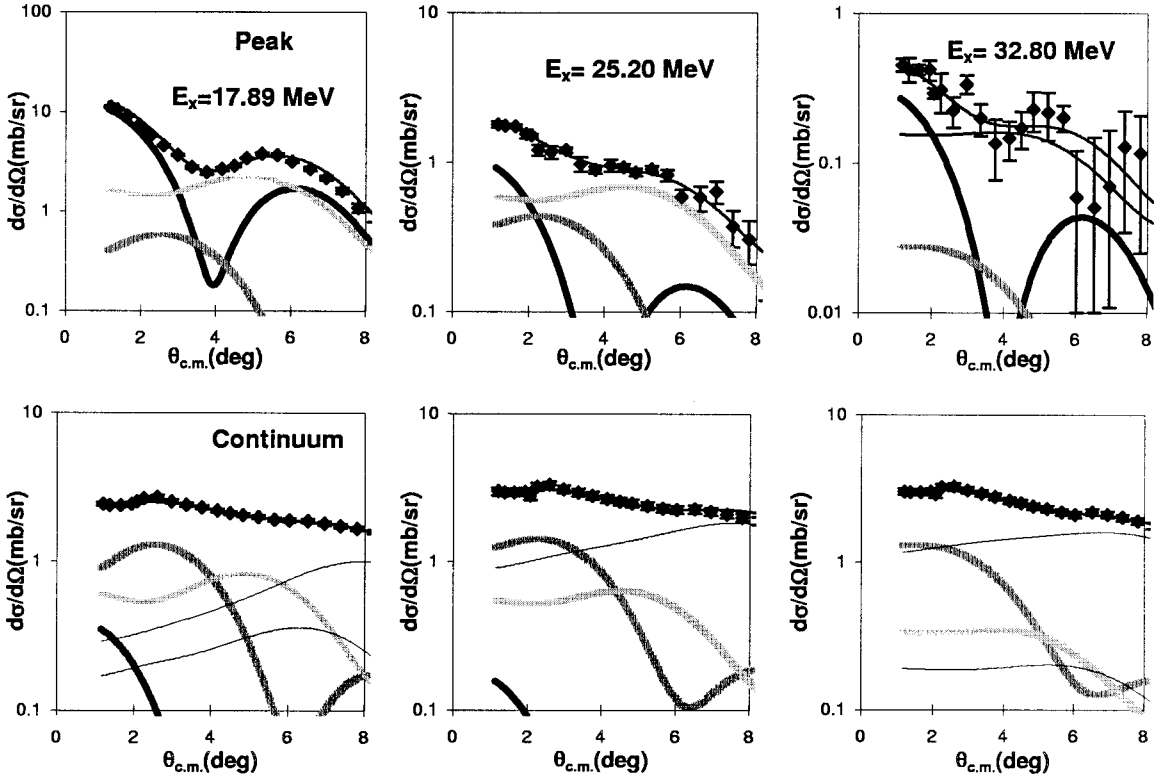

FIG. 4. Angular distributions obtained for inelastic α scattering for three excitation ranges of the GR peak and the continuum in ^{28}Si. Each bin is 316 keV wide and the average energies for each bin are shown. Thin lines through the data show the fits. The $E0$ contribution is shown by the thick black line, the isoscalar $E1$ contribution by the thick dark gray line, and the $E2$ contributions by the thick light gray line. $E3$ and $E4$ contributions are shown by thin lines. When not shown, errors are smaller than the data points.

tained in Ref. [3], normalized by the ratio given in Table II for each multipolarity, are shown superimposed. The $E0$ distribution shown in the top panel of Fig. 5 corresponds to $81\pm10\%$ of the $E0$ EWSR compared to $54\pm6\%$ reported in Ref. [3]. The additional strength seen in this measurement comes from the DWBA factor shown in Table II, the strength seen at low excitation (below the threshold of the measurement reported in Ref. [3]), the inclusion of $E0$ strength from what we call the continuum (it was not included in Ref. [3]), and the strength seen above $E_x=35$ MeV where the much better statistics of this measurement improved the analysis.

The $E2$ strength observed corresponds to $68\pm9\%$ of the $E2$ EWSR with a centroid of 18.54 MeV. Previous studies [3,18] identified approximately $32\pm5\%$ of the EWSR strength centered around 19.0 MeV. In this measurement, additional $E2$ strength was identified below the threshold of the measurement reported in Ref. [3] and from $25<E_x<35$ MeV. As can be seen from Table II, renormalizing by the deformed potential/folding model cross section would increase the strength reported in Ref. [3] to $40\pm6\%$ of the EWSR.

Isoscalar $E1$ strength (shown in the third panel of Fig. 5) corresponding to $15\pm4\%$ of the $E1$ EWSR was identified in the peak with a centroid of 19.2 ± 0.6 MeV and an rms width of 6.9 MeV. Generally the distribution is in excellent agreement with the renormalized distribution from Ref. [3]. Additional strength is seen in this measurement below the threshold of Ref. [3]. In addition to the deformed potential/folding correction shown in Table II, the calculation for $E1$ cross section used in Ref. [3] was a factor of 1.6 too low due to a numerical error, so that the $E1$ strength reported in Ref. [3] was in error by a factor of 1.6.

DISCUSSION

Kolomiets *et al.* [19] have calculated isoscalar $E0$ and $E2$ distributions in ^{28}Si, ^{40}Ca, ^{58}Ni, and ^{116}Sn as well as microscopic transition densities in HF-RPA using the SL1 Skyrme interaction, then used elastic scattering data to obtain folding model parameters consistent with the calculated mass distributions, and used these to calculate cross sections for 240 MeV inelastic scattering using a density dependent folding model with the microscopic transition densities. For ^{28}Si, Shlomo *et al.* [20] have improved the treatment of the continuum and recalculated $E0$ and $E2$ distributions as well as the isoscalar $E1$ distribution. The top three panels in Fig. 6 compare the cross sections obtained at the first peak in the angular distributions by Shlomo *et al.* to cross sections for each multipole obtained from the strength distributions shown in Fig. 5. The calculated distributions lie at higher excitation than the data and do not reproduce the structure in the data, particularly for $E0$ and $E2$. Kamerzdhiev *et al.* [21] have shown that in ^{40}Ca and ^{58}Ni, structure seen in the data can be reproduced if $1p1h$-phonon coupling is included, which was absent from the calculations of Shlomo *et al.* Centroids of the $E0$ and $E1$ distributions are sensitive to the

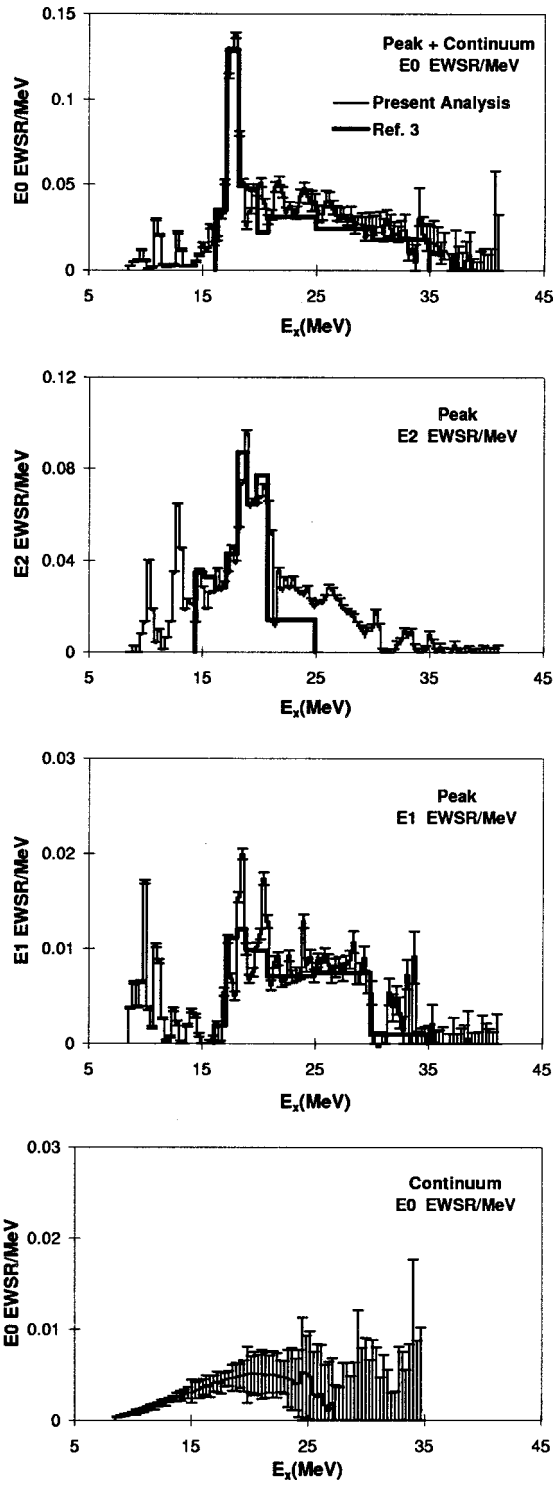

FIG. 5. Strength distributions obtained are shown by the histograms. Error bars represent the uncertainty due to the fitting of the angular distributions as described in the text. The thick black lines show the results from Ref. [3] normalized by the DWBA ratio from Table II.

nuclear compressibility, while the $E2$ distribution is sensitive to the effective mass and it would be interesting to see results with other interactions. The calculated $E1$ cross section significantly exceeds the measured cross section at higher excitation, suggesting that there may be considerably more $E1$ strength at higher excitation than obtained in our analysis of the giant resonance peak, which is consistent with our identification of only 15% of the $E1$ EWSR. The bottom panel in Fig. 6 shows the cross section for the sum of the $E1$ strength found in the peak and 30% of the strength found in the fits to the continuum compared to the Shlomo *et al.* calculation, shifted to lower excitation by 2 MeV. The agreement is relatively good from $E_x = 15$ MeV to the upper limit of our data at 40 MeV, suggesting that some of the $E1$ strength obtained from the analysis of the continuum is real and that there may be $E1$ strength above the range of our experiment.

K_A calculated for ^{16}O, ^{24}Mg, ^{28}Si, ^{40}Ca, ^{90}Zr, ^{116}Sn, ^{144}Sm, and ^{208}Pb for several interactions using the relativistic mean field parametrization of Chossy and Stocker [9] are shown compared to K_A obtained from the experimental data for these nuclei in Fig. 7. It can be seen that the parameter set NLC which corresponds to $K_{nm} = 224.5$ MeV gives K_A in reasonable agreement with the data over the entire range. Both NLC and NL1 predict E_{GMR} in excellent agreement with the ^{24}Mg and ^{28}Si data and within errors for ^{40}Ca, however, NL1 is low for mass 90 and higher. K_A obtained with the other parameter sets systematically miss all the data. A K_{nm} of 225 MeV is in agreement with $K_{nm} = 231 \pm 5$ MeV obtained [2] comparing the data for heavier nuclei with nonrelativistic calculations by Blaizot *et al.* [1] using the Gogny interaction.

Of course the agreement may be misleading, because the observed strength in ^{28}Si is 2σ from 100% and in ^{24}Mg is 3σ from 100% so that there may be missing strength which would significantly alter E_{GMR} for these nuclei. On the other hand, this may indicate we have seen all of the strength, but something in our estimate of the strength such as the use of a collective transition density has lead to an underestimate. The errors include only experimental errors and do not include uncertainties in predictions of the cross sections with the DWBA. The presence of such uncertainties and the difficulties in estimating them were discussed by Satchler and Khoa [14]. The calculations by Shlomo *et al.* of cross sections for $E0$ strength using microscopic transition densities do not agree well with the data, but also do not show $E0$ strength outside of the region where it is seen in this experiment, suggesting this experiment may have identified all of the $E0$ strength in ^{28}Si.

The Thomas-Fermi calculations of E_{GMR} by Wang, Chung, and Santiago [11] agreed relatively well with the data available at that time. However, there was a systematic underestimate of the GMR energy [2] in the data (from Ref. [6]) used by Wang, Chung, and Santiago. In Ref. [6] and all earlier works the centroid of the cross section was treated as the centroid of the strength distribution, a correction that at the time was smaller than the (substantial) errors on the centroid. With the recent precise data [2] this correction is important. Also, for nuclei with $A < 90$ only a small portion of the $E0$ strength had been found, mostly at lower excitation, resulting in GMR energies considerably below those now known. The calculations by Wang, Chung, and Santiago [11] of E_{GMR} are compared to the new data in Fig. 8, where it can be seen that their calculations underestimate the GMR energy in ^{208}Pb, ^{90}Zr, and ^{40}Ca. Their result is also well below

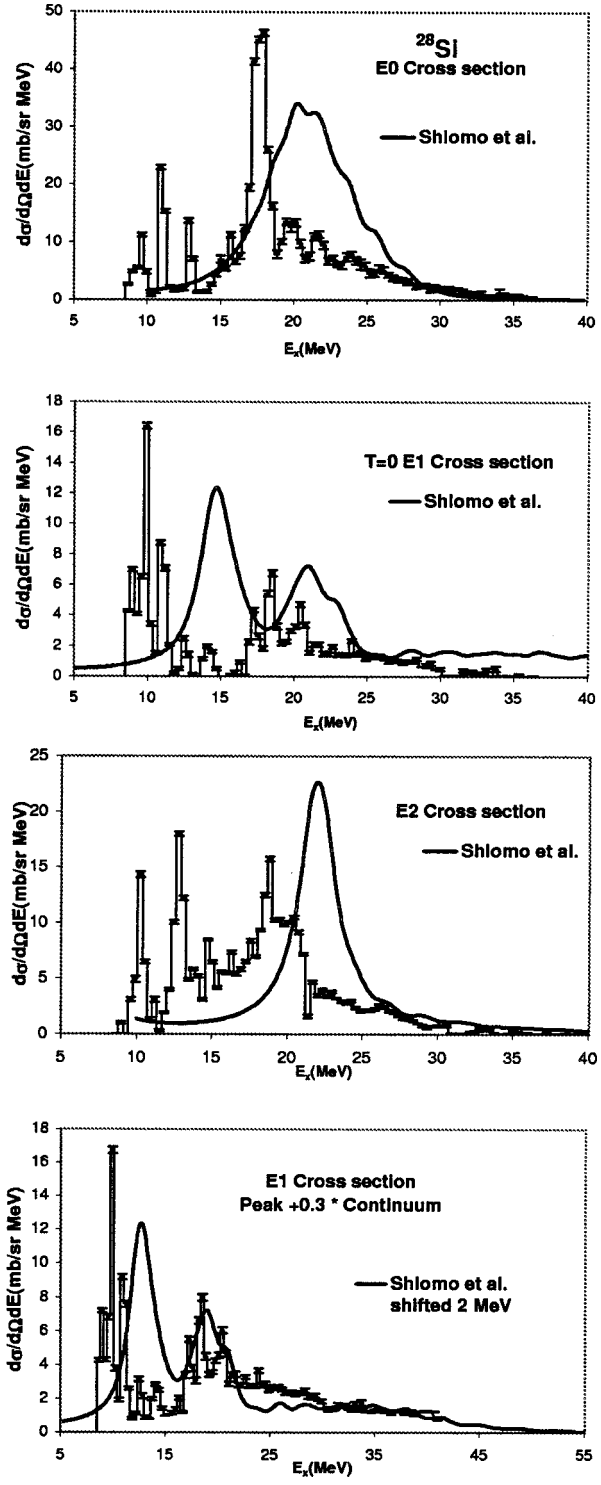

FIG. 6. The top three panels show cross sections at the first maximum in the angular distributions for $E0$, $E1$, and $E2$ excitation obtained from the strength distributions in Fig. 5 compared to those obtained by Shlomo *et al.* [20]. The fourth panel shows a sum of the $E1$ cross section from the second panel and 30% of the isoscalar $E1$ cross section from the analysis of the continuum compared to the calculations of Shlomo *et al.* [20] which have been shifted to lower excitation by 2 MeV. The error bars represent the uncertainty in the strength distributions shown in Fig. 5.

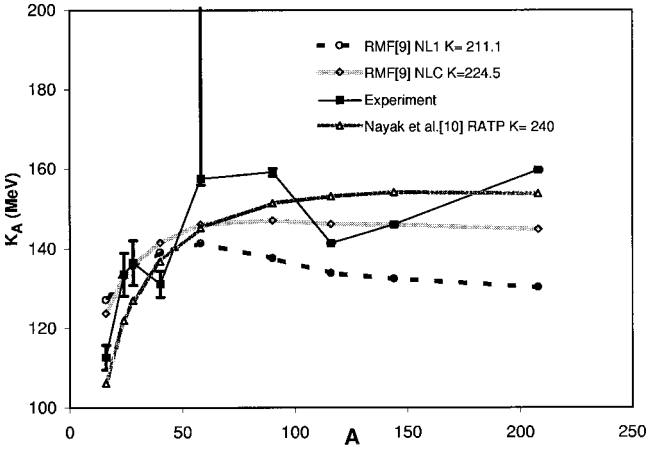

FIG. 7. Relativistic mean field calculations of K_A by Chossy and Stocker [9] for NL1 and NLC interactions and calculations of K_A using the RATP interaction by Nayak *et al.* [10] are shown superimposed on K_A extracted from the GMR energies.

the observed strength in ^{16}O [12], though less than half of the $E0$ EWSR strength has been identified in ^{16}O. Wang, Chung, and Santiago [11] include an anharmonicity correction to E_{GMR} which lowers the energy by 50 keV in ^{208}Pb, 700 keV in ^{40}Ca, and 2.6 MeV in ^{16}O. The trend of the data is much better reproduced without the anharmonicity term. Their calculations suggest that E_{GMR} should be about constant below $A=40$ due to the anharmonicity term that lowers E_{GMR} for lighter nuclei, whereas the experimental values continue to rise essentially as fast as the calculated energies without the anharmonicity correction. Blaizot *et al.* [1] also discuss the need for a significant anharmonicity term in lighter nuclei, and their result for ^{40}Ca including the anharmonicity term is in good agreement with the experimental result [4].

Also shown in Fig. 8 are calculations using parameters for the Leptodermous expansion obtained by Nayak *et al.* [10] using the SkM* interaction. Wang *et al.* showed that the Nayak *et al.* parameters for SkM* resulted in nuclear com-

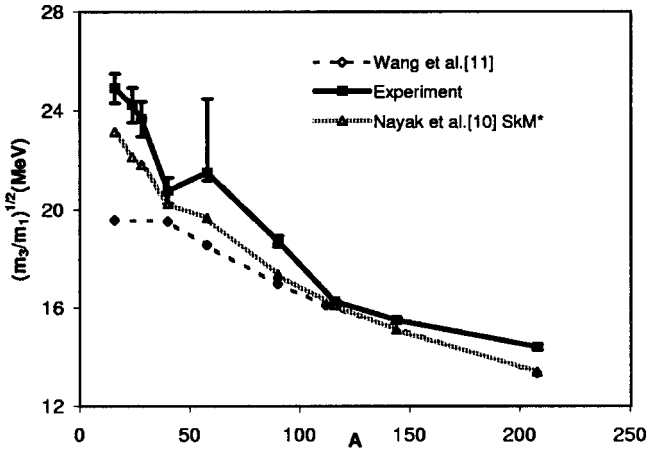

FIG. 8. Breathing mode energies obtained with Thomas-Fermi calculations by Wang *et al.* [11] with anharmonicity corrections and RPA calculations [10] with the SkM* interaction are shown superimposed on the data.

pressibilities (K_A) very similar to their Thomas-Fermi calculations. The energies calculated with the Nayak *et al.* parameters obtained from the SkM* interaction are systematically below the data, however those calculated with parameters from the RATP interaction (Fig. 7) fit the data well. For the RATP interaction, $k_{nm}=240$ MeV, which is in reasonable agreement with the results from Blaizot *et al.* [1], where interpolating between Gogny interactions suggests [2] that $K_{nm}=231$ MeV would reproduce the data well for $40<A<208$.

Chossy and Stocker, Wang *et al.*, and Nayak *et al.* worked within the scaling model which has been shown [7] for heavier nuclei to give transition densities very similar to those from RPA. That was not true in lighter nuclei [22], so that the justification for the scaling model is weaker in the lighter nuclei.

CONCLUSIONS

With the use of folding model calculations where B(EL) values obtained from inelastic α scattering for discrete 2^+ and 3^- states agree with electromagnetic values $81\pm10\%$, $68\pm9\%$, and $15\pm4\%$ of the isoscalar $E0$, $E2$, and $E1$ sum rules, respectively, were identified between $8\text{ MeV}<E_x<40$ MeV in ^{28}Si. The mass dependence of the compression modulus of finite nuclei from $A=24$ to 208 is reasonably well reproduced in relativistic mean field calculations with the NLC interaction having $K_{nm}=225$ MeV and in nonrelativistic calculations with the RATP interaction having $K_{nm}=240$ MeV, and over the range $A=40$ to 208 with the Gogny interaction with $K_{nm}=231$ MeV, but Thomas-Fermi calculations having $K_{nm}=234$ MeV are systematically low. The anharmonicity correction in the Thomas-Fermi calculation widens the disagreement for monopole resonance energies in light nuclei. There remains the question of whether 100% of the strength has been identified in ^{24}Mg and ^{28}Si (if not the energy moments could be substantially changed), however, a comparison of the calculations by Shlomo *et al.* of cross sections for $E0$ strength using microscopic transition densities to the data suggests that all of the $E0$ strength in ^{28}Si may have been identified. The comparison with the Shlomo *et al.* calculations for isoscalar $E1$ strength suggest that at higher excitation a substantial portion of the isoscalar $E1$ strength is in what we call the continuum. Calculations including $1p1h$-phonon coupling to explore the fragmentation of isoscalar strength and those using other interactions which might shift the centroids of the strength could be very informative.

ACKNOWLEDGMENTS

We thank S. Shlomo, B. Debresch, A. I. Sanzhur, and A. Moalem for making their calculations available to us before publication. This work was supported in part by the U.S. Department of Energy under Grant No. DE-FG03-93ER40773 and by The Robert A. Welch Foundation.

[1] J. P. Blaizot, J. F. Berger, J. Dechargé, and M. Girod, Nucl. Phys. **A591**, 435 (1995).
[2] D. H. Youngblood, H. L. Clark, and Y.-W. Lui, Phys. Rev. Lett. **82**, 691 (1999).
[3] D. H. Youngblood, H. L. Clark, and Y.-W. Lui, Phys. Rev. C **57**, 1134 (1998).
[4] D. H. Youngblood, Y.-W. Lui, and H. L. Clark, Phys. Rev. C **63**, 067301 (2001).
[5] D. H. Youngblood, Y.-W. Lui, and H. L. Clark, Phys. Rev. C **60**, 014304 (1999).
[6] S. Shlomo and D. H. Youngblood, Phys. Rev. C **47**, 529 (1993).
[7] J. P. Blaizot, Phys. Rep. **64**, 171 (1980).
[8] J. M. Pearson, Phys. Lett. B **271**, 12 (1991).
[9] T. v. Chossy and W. Stocker, Phys. Rev. C **56**, 2518 (1997).
[10] R. C. Nayak, J. M. Pearson, M. Farine, P. Gleissl, and M. Brack, Nucl. Phys. **A516**, 62 (1990).
[11] C. S. Wang, K. C. Chung, and A. J. Santiago, Phys. Rev. C **55**, 2844 (1997).
[12] Y.-W. Lui, H. L. Clark, and D. H. Youngblood, Phys. Rev. C **64**, 064308 (2001).
[13] J. R. Beene, D. J. Horen, and G. R. Satchler, Phys. Lett. B **344**, 67 (1995).
[14] G. R. Satchler and Dao T. Khoa, Phys. Rev. C **55**, 285 (1997).
[15] M. N. Harakeh and A. E. L. Dieperink, Phys. Rev. C **23**, 2329 (1981).
[16] P. M. Endt, Nucl. Phys. **A251**, 1 (1990). Data extracted from the ENSDF database, version (90), NNDC.
[17] S. S. Dietrich and B. L. Berman, At. Data Nucl. Data Tables **38**, 199 (1988).
[18] Y.-W. Lui, J. D. Bronson, C. M. Rozsa, D. H. Youngblood, P. Bogucki, and U. Garg, Phys. Rev. C **24**, 884 (1981).
[19] A. Kolomiets, O. Pochivalov, and S. Shlomo, Phys. Rev. C **61**, 034312 (2000).
[20] S. Shlomo, B. Debresch, A. I. Sanzhur, and A. Moalem (private communication).
[21] S. Kamerdzhiev, J. Speth, and G. Tertychny, Eur. Phys. J. A **7**, 483 (2000).
[22] K. Goeke, Phys. Rev. Lett. **38**, 212 (1977).